



Analysis of Dynamics in Cellular Neural Network

メタデータ	言語: eng 出版者: 公開日: 2010-04-06 キーワード (Ja): キーワード (En): 作成者: Tsubata, Toshihide, Kawabata, Hiroaki, Takeda, Yoji メールアドレス: 所属:
URL	https://doi.org/10.24729/00008357

Analysis of Dynamics in Cellular Neural Networks

Toshihide TSUBATA*, Hiroaki KAWABATA**,
and Yoji TAKEDA**

(Received October 30, 1993)

Cellular neural network (CNN) with an external oscillating input has complex oscillations such as chaos, quasi-periodicity and intermittency. It also shows a phenomenon of an attractor switching for the unsymmetric template. This paper describes these oscillations and phenomena when an amplitude of the external input is changed. These oscillations in the CNN may show a possibility of dynamic information-processing system.

1. Introduction

In order to achieve a human-like operating of information processing, many studies have been made with the neural networks. Neural networks are parallel information processing systems and "cellular neural networks" (CNN's) proposed by L.O.Chua and L.Yang are one of them^{1),2)}. A CNN is made up of regularly spaced clone circuit, called cell, which connects with only its neighbors, and this neural network has a possibility for the applications such as image processing or pattern recognition system. Connection weights between one cell and the others are described by a "cloning template" which specifies the dynamic rule of the cellular neural network. Depending on the values of cloning template and the initial state, the various steady state performances appear^{1),2),4),5),6)}. At present, studies about cellular neural networks have been done from the point of view of applying its stable steady states, which arise when the symmetric template is chosen. In the meanwhile, when an unsymmetric cloning template is chosen, the dynamics does not always show a complete stability and a chaotic oscillation arises. Although it is difficult to use the chaotic oscillation for the information processing, the amount of information which is included in the time series is greater than that of the static states. The analysis for the chaotic phenomena included in the CNN is insufficient at the present time³⁾.

In this paper, we examine the dynamics of the chaotic oscillations included in the cellular neural networks. It is recognized that a variety of oscillation forms, such as periodicity, quasi-periodicity, intermittency, chaos, and attractor switching (attractor merging) can be included in the CNN for an unsymmetric cloning template when the amplitude of a periodic external input is changed.

* Sharp Co. Ltd.

** Department of Electrical and Electronic Systems, College of Engineering.

2. Model equation

In general, a cellular neural network is composed of an $m \times n$ matrix cell neurons in which the governing equation of the ij -th cell neuron is given by the following differential equation:

$$\dot{x}_{ij} = -x_{ij} + A * y_{ij} + B * u_{ij} + I, \tag{1}$$

$$(1 < i < m, 1 < j < n)$$

where x_{ij} and u_{ij} are the state variable and input of the ij -th cell neuron. I_{ij} stand for the threshold value. A and B are the matrices which correspond to the connection weight coefficients, and they are called "templates". $A * y_{ij}$ and $B * u_{ij}$ are the interference terms of the outputs and inputs from the neighbor cells. The convolution operator $*$ is introduced to express the interference terms with compact forms.

$$A * y_{ij} = \begin{bmatrix} a_{-r, -r} & \cdots & a_{-r, 0} & \cdots & a_{-r, r} \\ \vdots & \ddots & \vdots & \ddots & \vdots \\ a_{0, -r} & \cdots & a_{0, 0} & \cdots & a_{0, r} \\ \vdots & \ddots & \vdots & \ddots & \vdots \\ a_{r, -r} & \cdots & a_{r, 0} & \cdots & a_{r, r} \end{bmatrix} * y_{ij} \tag{2}$$

$$= a_{-r, -r}y_{i-r, j-r} + \cdots + a_{-r, 0}y_{i-r, j} + \cdots + a_{-r, r}y_{i-r, j+r} + \cdots$$

$$+ a_{0, -r}y_{i, j-r} + \cdots + a_{0, 0}y_{ij} + \cdots + a_{0, r}y_{i, j+r} + \cdots$$

$$+ \cdots$$

$$+ a_{r, -r}y_{i+r, j-r} + \cdots + a_{r, 0}y_{i+r, j} + \cdots + a_{r, r}y_{i+r, j+r} + \cdots$$

Output y_{ij} is given by the following function of state x_{ij} .

$$y_{ij} = \frac{1}{2} (|x_{ij} + 1| - |x_{ij} - 1|). \tag{3}$$

As mentioned in introduction, we focus on the chaotic dynamics included in CNN, so here we deal with a simple, one-dimensional spaced, cellular neural network which is composed of only two neurons in Fig. 1³⁾. The dynamics is described as follows;

$$\begin{bmatrix} \dot{x}_1 \\ \dot{x}_2 \end{bmatrix} = \begin{bmatrix} -1 & 0 \\ 0 & -1 \end{bmatrix} \begin{bmatrix} x_1 \\ x_2 \end{bmatrix} + \begin{bmatrix} p & -s \\ s & p \end{bmatrix} \begin{bmatrix} y_1 \\ y_2 \end{bmatrix} + \begin{bmatrix} 1 & 0 \\ 0 & 1 \end{bmatrix} \begin{bmatrix} g(t) \\ 0 \end{bmatrix} + \begin{bmatrix} 0 \\ 0 \end{bmatrix} \tag{4}$$

where p is the feedback connection weight of a cell's output, s is the connection weight from the neighbor cell, and $g(t)$ is the external periodic force. In this case, the template is described as $(s, p, -s)$. The external input $g(t)$ and the output function $f(x)$ is described as follows;

$$g(t) = A_m \sin(2\pi t/T) \tag{5}$$

$$f(x_i) = y_i = \frac{1}{2} (|x_i + 1| - |x_i - 1|). \tag{6}$$

Where A_m is the amplitude and T is a period of the external input.

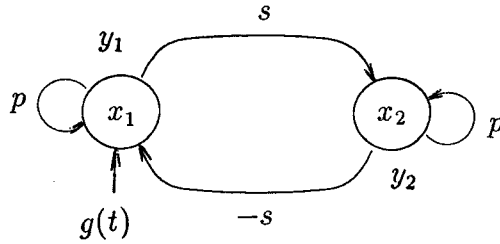
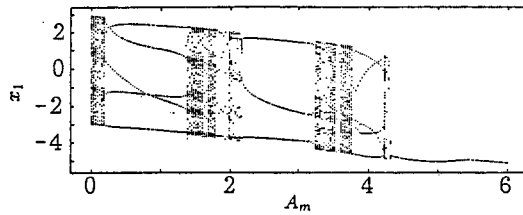


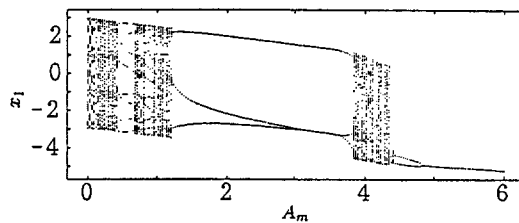
Fig.1 Simple model of CNN with an external input

3. Simulation results and discussions

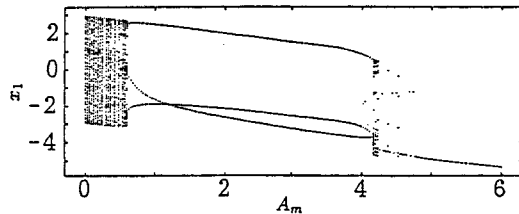
Varying the amplitude A_m of the sinusoidal input $g(t)$ as a controlling parameter, various dynamics can be recognized. Fig.2 shows the bifurcation diagrams of x_1 for $s=1.1, 1.2,$ and 1.3 using the Runge-Kutta method with a time step $\Delta t = 0.05$, and the initial conditions as $x_1(0) = 0.25$ and $x_2(0)=0.15$. Among them, we focus on Fig.2(b) for $s = 1.2$ and discuss the dynamics. A chaotic attractor can be observed around $A_m=4.0$.



(a) $s = 1.1$



(b) $s = 1.2$



(c) $s = 1.3$

Fig.2 Bifurcation diagram of x_1

3-1. Quasi-periodicity

Quasi-periodic attractors can be recognized for the small value of A_m . The representative quasi-periodic attractors for $A_m = 0.69$ and $A_m = 1.20$ are given in Fig. 3(a) and Fig. 3(b), respectively. These two figures are shown by the Poincaré sections of (x_1, x_2) . We also show Lyapunov exponents in Fig. 4(a) and Fig. 4(b) for $A_m = 0.69$ and $A_m = 1.20$, respectively, and both the largest Lyapunov exponents are 0.00, which represents the quasi-periodicity.

The first return map (circle map) of a flow on T^2 (2-torus) can be described by a continuous and invertible mapping. The quasi-periodic state can be analysed in more detail by examining this circle map. Fig. 5(a) and Fig. 5(b) are circle maps for $A_m = 0.69$ and for $A_m = 1.20$, respectively. These maps describe the rotating motion on the section of 2-torus. The circle map is a monotonically increasing (or decreasing) function, and has two fictitious discontinuities due to the identification of 0 and 2π on the circle. A value of θ_n is a rotating angle for n -th mapping on the Poincaré section of Fig. 3.

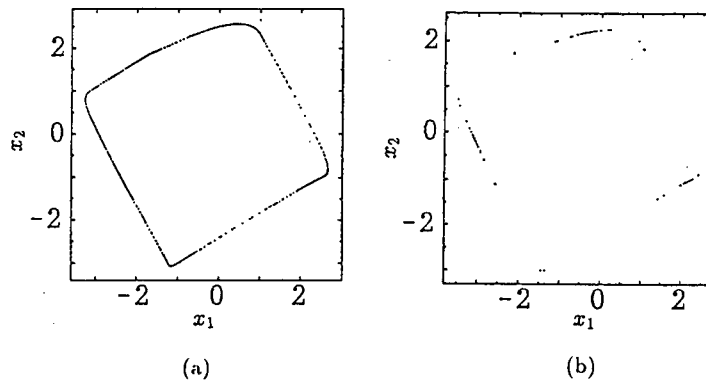


Fig. 3 Quasi-periodic attractor on Poincaré section of (x_1, x_2)

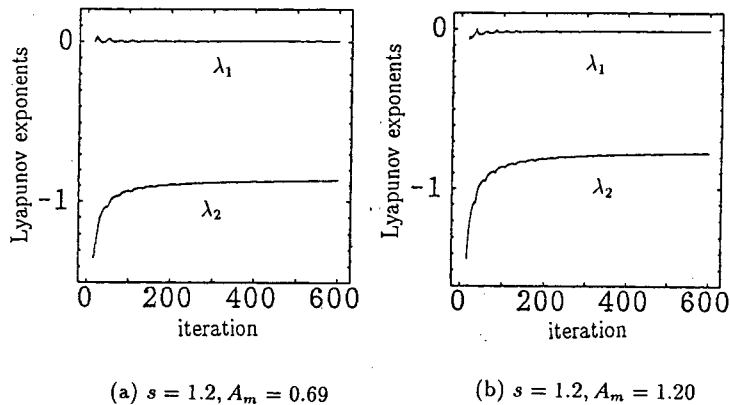


Fig. 4 Lyapunov exponents (λ_1, λ_2)

A rotation number can characterize such a mapping on the circle. When this number is rational, we have a frequency-locking. In the meanwhile, a quasi-periodic behavior can be seen when this number is irrational. Here, rotation number ρ is defined as follows;

$$\rho = \lim_{n \rightarrow \infty} \frac{\theta_n - \theta_0}{n} \pmod{2\pi}. \quad (7)$$

We calculate this number for each value of A_m and show the following table.1 which represents frequency-locking or quasi-periodic state. When $A_m = 1.20$, we have $\rho = 0.319$. Because this number is close to $1/3$, there are three zones of the greatest density in Fig.2(b) and Fig.5(b), and these zones foreshadow a frequency-locking of order three. The power spectrum of x_i for $A_m = 1.20$ in Fig.6 also shows the quasi-periodic regime with two frequencies f_1 and f_2 . In this case, we have a sampling frequency $f_s = 0.25$. A value of f_1/f_2 is 3.125, and this result also explains the existence of three zones of the greatest density in Fig.3(b) and Fig.5(b).

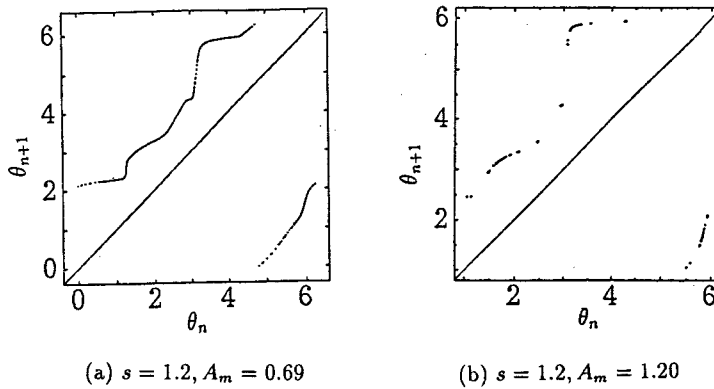


Fig. 5 Circle map

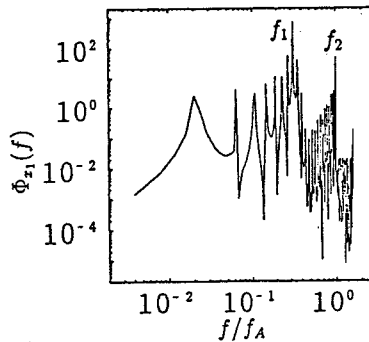


Fig. 6 Power spectrum of x_i for $A_m = 1.20$.

3-2. Intermittency

After the phase-locking state, quasi-periodic attractor becomes chaos via intermittency. There are three types of intermittency, which are called type-I, type-II and type-III. Type-I intermittency is associated with the saddle-node bifurcation of the limit cycle, type-II with a subcritical Hopf bifurcation, and type-III with a subcritical period-doubling bifurcation^{7),8),9),10)}.

Fig. 7(a)~(c) show an output x_2 , and a route to chaos in this case is an intermittent one. A three-periodic oscillation changes into chaos via this intermittency. In order to classify this intermittency, we show three fold circle maps in Fig. 8. From these figures, a saddle-node bifurcation is observed and we recognize that this intermittency can be classified as type-I.

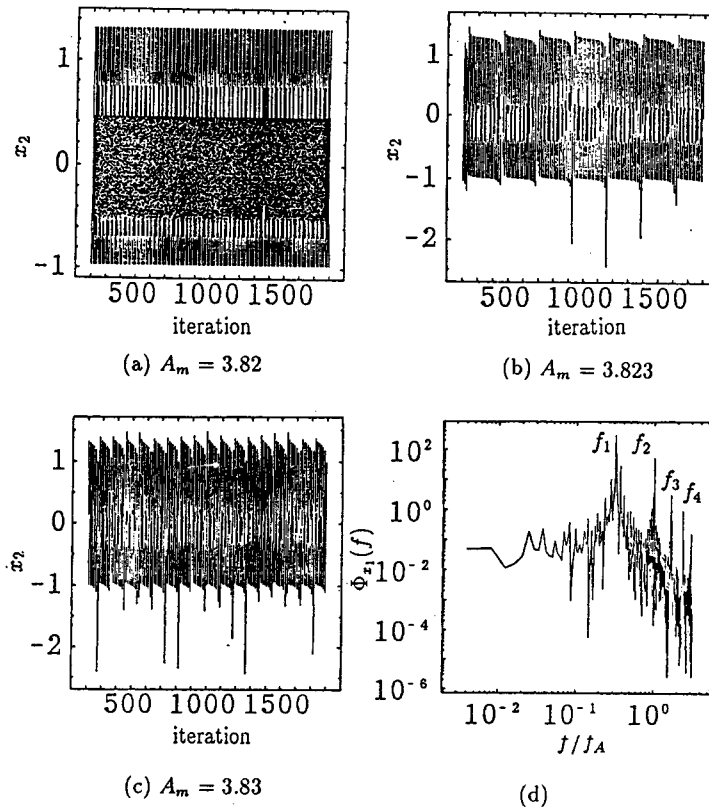


Fig. 7 Time series of output x_2

We consider the return map which produces a type-I intermittency. In general, this return map is described as follows[7];

$$I_{n+1} = f(I_n) = r + I_n + aI_n^2 \quad (8)$$

where a is constant and r is a parameter. When r is negative, $\text{map}(6)$ has two fixed points. These stability is controlled by $f'_r(I_n)=1+2aI_n$ and one of them is stable, which corresponds to the stable periodic oscillation before the onset of intermittency, and the other point is unstable. When $r = 0$, the two fixed points merge into semi-stable fixed point. When r is positive, fixed points disappear and there is a narrow channel between the diagonal and the graph of $f_r(I_n)$, and this case corresponds to the saddle-node bifurcation shown in Fig. 8. The trajectory travels slowly through the channel from positive value of $\theta(n)$ to negative value of $\theta(n)$ in Fig. 8. This narrow channel produces the laminar behavior of the intermittent state, and the regular pulsing period is called "laminar length".

Table 1 Dynamical state with the rotation number and the largest Lyapunov exponent for each value of A_m

A_m	rotation number	largest Lyapunov exponent	dynamical state
0.25	0.238	0.00	quasi-periodic
0.45	0.250(=4/16)	-0.02	4:16 frequency-locking
0.69	0.254	0.00	quasi-periodic
0.85	0.273(=11/40)	-0.04	11:40 frequency-locking
1.00	0.284(=7/25)	-0.03	7:25 frequency-locking
1.20	0.319	0.00	quasi-periodic
2.00	0.333(=3/9)	-0.18	3:9 frequency-locking

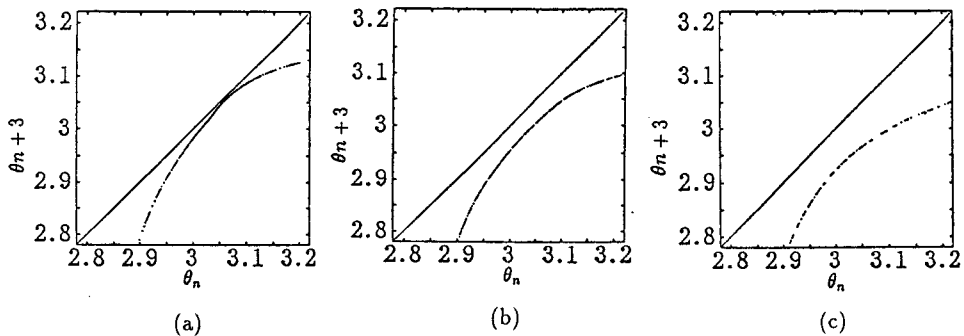


Fig. 8 Three fold circle map

To clarify this type of intermittency further, we show a distribution of the laminar length for $A_m = 3.83$ in Fig. 9. The distribution of type-I shows a maximum for long laminar length, but that of type-II or type-III is exponentially falling towards long length[7]. From this distribution nature of the laminar lengths, we also conclude that intermittency in this case is type-I.

After this intermittent state, a "weak" chaotic attractor can be observed for $A_m = 3.88$. For $A_m = 3.88$, Fig. 10(a) shows a Poincaré map, Fig. 10(b) a phase-plane trajectory of state variables x_1 and x_2 . The largest Lyapunov exponent in this case is 0.04. This attractor corresponds to a frame of the "lady's shoe attractor" [3], which we will show in the next section.

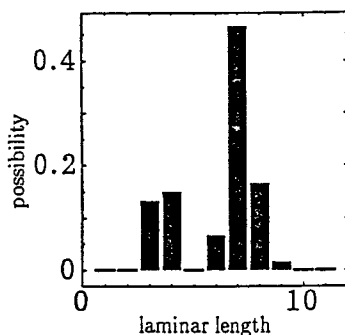


Fig. 9 Distribution of the laminar lengths for $A_m = 3.83$

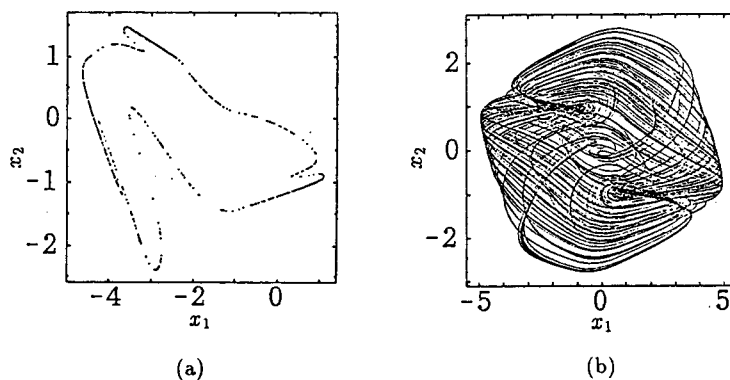


Fig. 10(a) “Weak” chaotic attractor on Poincaré section of (x_1, x_2) for $A_m = 3.88$.

Fig. 10(b) Phase-Plane trajectory of state variables x_1 and x_2 of a “weak” chaotic attractor for $A_m = 3.88$.

3-3. Period doubling, attractor switching, and chaotic attractor

Period doublings can be seen for the relatively large value of A_m . We show these bifurcations in Poincaré maps of Fig. 11(a)~(d). After the period doublings, a chaotic attractor which is shown in Fig. 12(a) and Fig. 12(b) is observed for $A_m = 4.37$. The largest Lyapunov exponent of this chaotic attractor is 0.14. In addition, if we choose the initial conditions as $x_1(0) = x_2(0) = -1.0$ for $A_m = 4.37$, we can observe another chaotic attractor shown in Fig. 12(c) and Fig. 12(d). That is to say, there exists two chaotic attractors in which each attractor has its own basin. And after the critical point, an orbit spends a long stretch of time in the region of one of two attractors Figs. 11(a),(b) and Figs. 11(c),(d), and after such a time stretch, the orbit spends a long stretch of time in the region of another attractor. Then, these two chaotic attractors merge into the “lady’s shoe attractor” of Fig. 13(a) and Fig. 13(b). Where

the largest Lyapunov exponent of this chaotic attractor is 0.16. In a time-series plot of the output x_2 , this switching (merging) is observed in Fig.14 for $A_m = 4.365$ when the initial conditions are $x_1(0) = 0.25$ and $x_2(0) = 0.15$. In that way, the “lady’s shoe attractor” is produced via attractor switching (attractor merging)[11]. If we take a value of A_m smaller, this “lady’s shoe attractor” becomes the weak chaotic attractor of Figs.10(a),(b). The larger a value of A_m becomes, The larger fractal dimension of “lady’s shoe attractor” becomes. It is one of our future problems to analyse these process in detail.

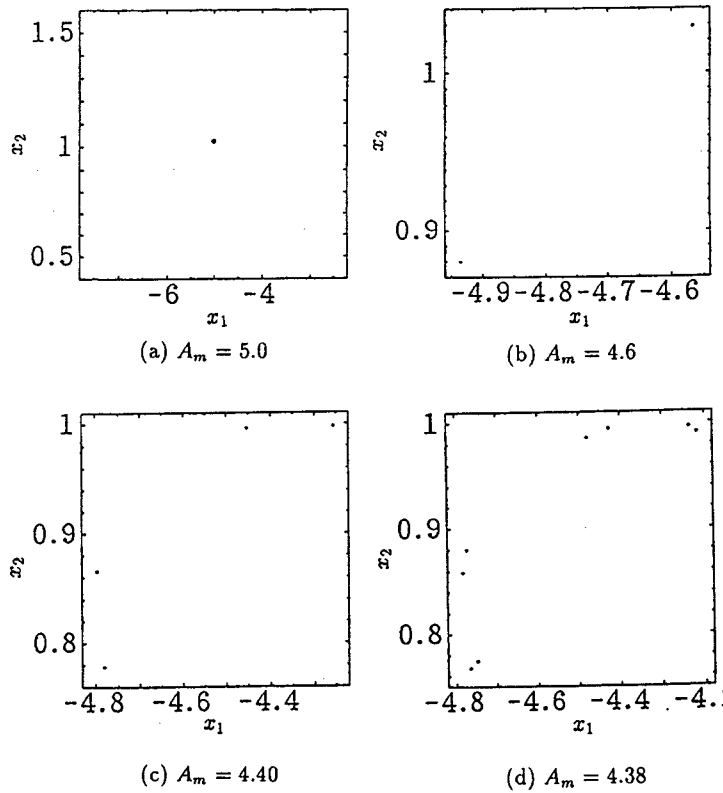


Fig. 11 Poincaré map

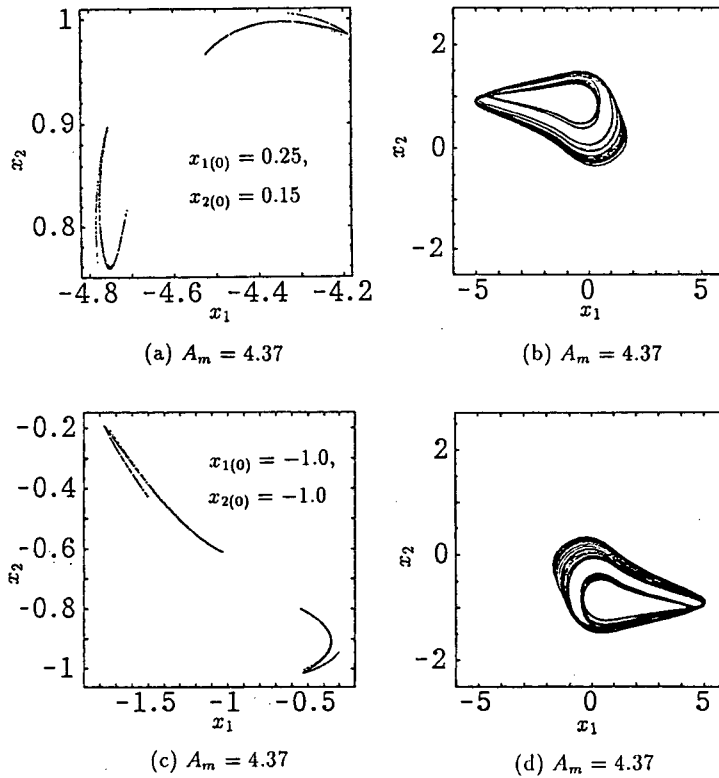


Fig. 12 Bifurcations in Poincaré section

- (a) Chaotic attractor on Poincaré section
- (b) Phase-plane trajectory of state variables x_1 and x_2
- (c) Chaotic attractor on Poincaré section
- (d) Phase-plane trajectory of state variables x_1 and x_2

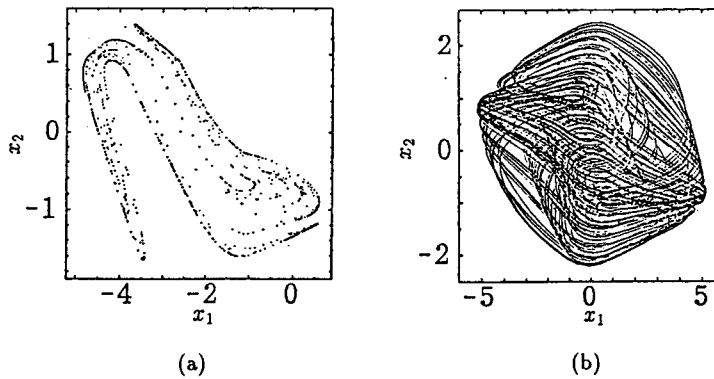


Fig. 13 The "lady's shoe attractor" for $A_m = 4.20$

- (a) Poincaré section
- (b) Phase-Plane trajectory

4. Conclusions

In this paper, we have studied about the complex dynamics in cellular neural networks with an external oscillating input. Periodicity, quasi-periodicity, intermittency, and chaos have been observed and these oscillations have been analyzed by using the Poincaré map, the power spectrum, the rotation number, the distribution of laminar lengths, and so on. Although it is known that there are some routes to chaos in many nonlinear dissipative systems, for example, the route of period doubling, quasi-periodic break down, and intermittency. We can observe all of these routes to chaos in the CNN. In section 3-1, the quasi-periodic attractor which is an almost three periodic frequency-locking, or some frequency-lockings can be observed, and after the frequency-locking, the quasi-periodic attractor becomes chaos via an intermittency. We have also discussed about the intermittency in section 3-2. The type of this intermittency is type-I which is associated with a saddle-nobe bifurcation, and this type is the same with *Onchidum* pacemaker neuron[8] except for the normal squid axons[9]. In section 3-3, periodic oscillations, period doublings, and the attractor switching can be observed. Although the attractor switching of chaos seems to be attractive in the aspect of its engineering applications, the analysis of the attractor switching is insufficient, and it is one of our future problems.

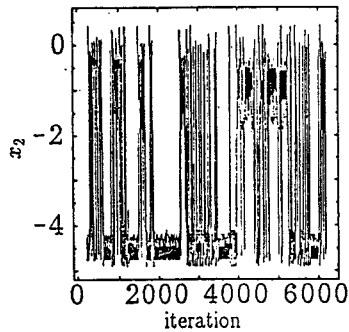


Fig. 14 Time series of x_2 for $A_m = 4.365$

Acknowledgments

One of the authors, T.Tsubata, would like to thank Prof. Masaya Hirata (Osaka Prefectural College of Technology) and Mr. Toshikuni Nagahara (Department of Electrical and Electronic Systems, College of Engineering) for their warm encouragement.

References

- [1] L. O. Chua and L. Yang: "Cellular Neural Networks: Theory", IEEE Trans. Circuits Syst., Vol. 35, No. 10 (1988)
- [2] L. O. Chua and L. Yang: "Cellular Neural Networks: Applications", IEEE Trans. Circuits Syst., Vol. 35, No. 10 (1988)
- [3] F. Zou and J. A. Nossek: "A Chaotic Attractor with Cellular Neural Networks", IEEE Trans. Circuits Syst., Vol. 38, No. 7 (1991)
- [4] L. O. Chua and T. Roska: "Stability of a Class of Nonreciprocal Cellular Neural Networks", IEEE Trans. Circuits Syst., Vol. 37, No. 12 (1990)
- [5] T. Matsumoto, L. O. Chua, and H. Suzuki: "CNN cloning template: Shadow Detector", IEEE Trans. Circuits Syst., Vol. 37, No. 8 (1990)
- [6] C. W. Wu, L. O. Chua, and T. Roska: "Two-Layer Radon Transform Cellular Neural Network" IEEE Trans. Circuits Syst., Vol. 39, No. 7 (1992)
- [7] P. Berge, Y. Pomeau, and C. Vidal: "Order within Chaos", Wiley, New York (1984)
- [8] H. Hayashi, S. Ishizuka, and K. Hirakawa: "Chaotic Responce of the Pacemaker Neuron", J. Phys. Soc. Jpn., 54 (1985)
- [9] G. Matsumoto, K. Aihara, et al.: "Chaos and phase locking in normal squid axons", Phys. Lett. A, 123 (1987)
- [10] T. Tsubata, H. Kawabata, et al.: "Intermittency of Recurrent Neuron and its Network Dynamics", IEICE Trans. Fundamentals, Vol. E76-A, No. 5 (1993)
- [11] C. Grebogi, E. Otto, F. Romeias, and J. A. Yorke: "Critical exponents for crisis-induced intermittency", Phys. Rev. A, Vol. 36, No. 11 (1987)